Isotope Ratios of Light Fragments as Thermometers in Heavy Ion Collisions

T. Möhlenkamp(2) for the ALADIN/LAND collaboration:

M. Begemann-Blaich,(1) Th. Blaich,(4) H. Emling,(1) A. Ferrero,(5)* C. Groß ,(1) G. Immé,(6) I. Iori,(5) G.J. Kunde,(1)† W.D. Kunze,(1) V. Lindenstruth,(1)‡ U. Lynen,(1) A. Moroni,(5) W.F.J. Müller,(1) B. Ocker,(3) J. Pochodzalla,(1) G. Raciti,(6) T. Rubehn,(1) H. Sann,(1) A. Schüttauf,(3) C. Schwarz,(1) W. Seidel,(2) V. Serfling,(3) J. Stroth,(1) W. Trautmann,(1) A. Trzcinski,(7) A. Tucholski,(7) G. Verde,(6) A. Wörner,(1) E. Zude,(1) and B. Zwieglinski(7)

(1)Gesellschaft für Schwerionenforschung, 64220 Darmstadt, Germany
(2)Forschungszentrum Rossendorf, 01314 Dresden, Germany
(3)Institut für Kernphysik,Universität Frankfurt, 60486 Frankfurt, Germany
(4)Institut für Kernchemie, Universität Mainz, 55099 Mainz, Germany
(5)Dipartimento di Fisica, Università di Milano and I.N.F.N., 20133 Milano, Italy
(6)Dipartimento di Fisica dell' Università and I.N.F.N., 95129 Catania, Italy
(7)Soltan Institute for Nuclear Studies, 00 681 Warsaw, Hoza 69, Poland

Abstract

Fragment distributions resulting from Au+Au collisions at an incident energy of E/A=600 MeV are studied. A temperature scale was derived from observed yield ratios of He and Li isotopes. The relation between this isotope temperature and the excitation energy of the system exhibits a behavior which is expected for a phase transition. The nuclear vapor regime takes over at an excitation energy of 10 MeV per nucleon, a temperature of 5 MeV and may be characterized by a density of 0.15-0.3 normal nuclear density.

1 The Quest for the Liquid-Gas Phase Transition

Stimulated by the van der Waals behavior of the nucleon-nucleon force [1, 2, 3] and supported by the observation of a power law for the produced fragments in proton induced

*On leave from the Comision Nacional Energia Atomica, Argentina
†Present address: National Superconducting Cyclotron Laboratory, Michigan State University, East Lansing, MI 48824, USA
‡Present address: Lawrence Berkeley Laboratory, Berkeley, CA 94720

collisions [4], the idea of a liquid-gas phase transition in nuclear matter emerged [1, 2, 5, 6, 7] and even speculations on a second order phase transition at the critical point [8] were raised [9, 10]. In the subsequent years, interest in this phenomenon faded once the universality - and the corresponding 'theory-invariance' - of the observed power law and the associated critical-point exponent τ emerged (see e.g. refs. [11, 12]). In the meantime, renewed interest arouse just because of the similarities between very different phenomena [13] and - most recently - because of the attempt to extract critical-point exponents of fragmenting nuclear systems produced in the interaction of 1 AGeV Au nuclei with a carbon target [14, 15].

Searching for signals of a nuclear phase transition, we are confronted with at least four complications which are inherent – albeit not specific – for nuclear systems:
(1) Nuclei are composed of a limited number of constituents. For finite systems a broadening of a phase transition [16, 17] and a reduction of the critical temperature from its bulk value of 15-20 MeV is expected [2, 17, 18, 19, 20].
(2) Nuclei are charged. The long-range Coulomb-repulsion between the constituent protons introduces instabilities [21] which may lead to a considerable shift of the critical temperature downwards to values around 5 MeV [3, 22, 23].
(3) Nuclei are transient systems without external field (e.g. pressure) and will, therefore, expand prior to their disassembly [7, 24, 25, 26, 27, 28]. Furthermore, the aggregation into clusters gives rise to an effective equation-of-state [29].
(4) Nuclei are closed systems without a heat bath. Consequently, the temperature of the system cannot be pre-determined but has to be reconstructed from observable quantities.

This contribution reports on a search for a signal of a phase transition in projectile spectators which are produced in Au+Au collisions at E/A=600 MeV. Special attention will be payed to the last of the four complications mentioned above, i.e. the temperature determination of nuclear systems.

2 Experimental Method

Generally phase transitions of rather small clusters (~10 constituents) are still well defined, distinguishable [17, 30, 31, 32] and even detectable [33]. Excited nuclei, however, are generated in energetic nucleus-nucleus collisions whose complex dynamical evolution may obscure or even destroy possible signals of a phase-transition. As discussed in more detail by W. Trautmann in his talk at this conference [37], spectator matter seems to be ideally suited to investigate a thermally-driven phase transition: As indicated by the universality of the projectile fragment distributions [34], the memory of the entrance channel dynamics is lost prior to the decay of the spectators and the radial flow dynamics, which was shown to affect the fragmentation process [35], is small in these systems [35, 36].

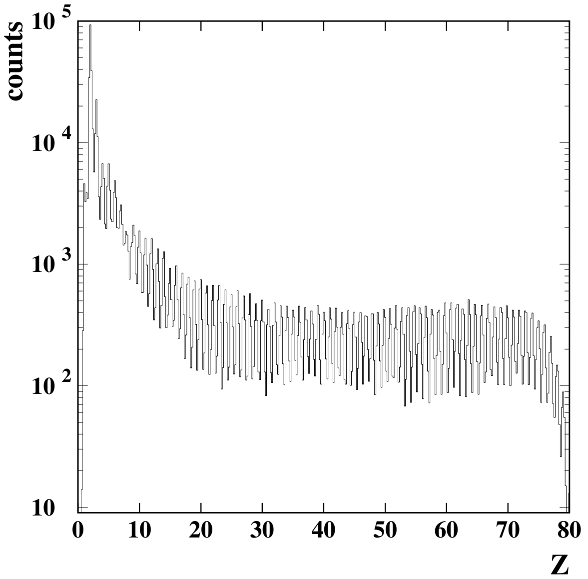

Figure 1: Combined charge spectrum measured with the TP-MUSIC detector and the TOF-Wall of the ALADIN forward spectrometer system.

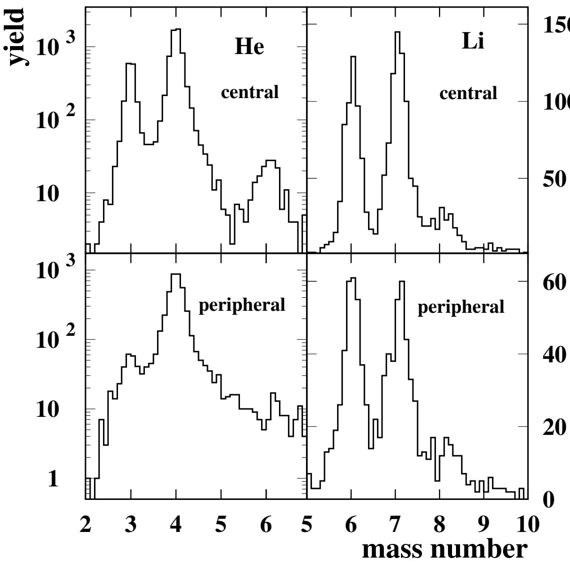

Figure 2: Mass spectra of He fragments (left panel) and Li fragments (right panel). The upper parts display central collisions while the lower parts show the distributions for peripheral collisions.

The experiment was performed with the ALADIN forward spectrometer system [38] of the GSI facility. Time-of-flight and charge information for fragments with Z$\geq$2 were provided by the TOF-wall with an efficiency close to 100%. The TP-MUSIC detector, equipped with 48 anode stripes and 18 multiwire proportional counters, allowed the measurement of the charges, positions and angles of fragments with Z$\geq$2. The charge identification capability of the ALADIN setup is illustrated in Fig. 1. Complete tracking information was obtained for 32% (70%) of all detected Z=2 (Z=10) particles. Combining this information with the time-of-flight measurement, the masses of light fragments were determined with a resolution of about ΔA_{FWHM}=0.3 (0.5) for Z=2 (Z=10) particles, respectively (Fig. 2).

Charged particles emitted beyond the acceptance of the ALADIN spectrometer were detected and separated according to Z in a 84 element Si-CsI(Tl) hodoscope placed in front of the magnet. Neutrons emitted from the projectile spectator were detected in the LAND detector [39]. In order to exclude particles from the participant region, an angular constraint of $\theta_{lab} \leq 7.3^o$ in the laboratory system and a rapidity cut corresponding to approximately 70% of the beam rapidity was applied to all detected charged fragments and neutrons.

3 The Isotope Thermometer

For a microcanonical ensemble, the thermodynamic temperature T of a system with total energy E may be defined in terms of the total-energy state density $\Omega(E)$ via the relation

$$\frac{1}{T(E)} = \frac{\partial\,(ln\Omega(E))}{\partial E}. \tag{1}$$

An experimental determination of the state density $\Omega(E)$ and its energy dependence is, however, hitherto impossible. Therefore, nuclear temperature determinations take recourse to 'simple' observables which constitute - at least for some ideal situations and generally within a canonical treatment - a good approximation to the true thermodynamic temperature. For example, for a nuclear system at low density and in chemical and thermal equilibrium a measure of the temperature T of the system may be obtained via double ratios of two isotope pairs (Y_1/Y_2) and (Y_3/Y_4) differing by the same number of neutrons and/or protons [40]:

$$R = \frac{Y_1/Y_2}{Y_3/Y_4} = a \cdot e^{[(B_1-B_2)-(B_3-B_4)]/T}. \tag{2}$$

Here, B_i denotes the binding energy of particle species i and the constant a contains known spins and mass numbers of the fragments. Of course, a meaningful temperature scale can only be derived if the ratio R is sufficiently sensitive to the temperature of the system and if the yields of the considered fragments are measurable over a large range of excitation energy. A large sensitivity of this thermometer may be achieved if the constant $b = (B_1 - B_2) - (B_3 - B_4)$ is larger than the typical temperature to be measured. In table 1 numerical values for the parameters a and b are listed for several isotope pairs. Particularly large values for b are obtained if a $^3He/^4He$ ratio is involved. Indeed, the large cross section of He fragments as a common substance of a 'liquid' and a 'vapor' regime of nuclear systems *and* the strong binding energy of the α-particle is the lucky coincidence which is the basis of the temperature determination presented hereafter. In order to acquire also for the second yield ratio a sufficient production yield we define in the following a temperature $T_{HeLi,0}$ in terms of the yield ratios ^{3}He/^{4}He and ^{6}Li/^{7}Li

$$T_{HeLi,0} := 13.33/ln(2.18 \cdot \frac{Y_{6Li}/Y_{7Li}}{Y_{3He}/Y_{4He}}). \tag{3}$$

Up to this point we considered nuclei in their ground state only and we ignored the effect of sequential decays during the final stage of the disassembly process. In particular, the yield of α-particles may be modified by secondary decays. (Note, however, that the effect of the α-feeding is partially neutralized by the feeding of ^3He.) Differentiating Eq.2,

1. ratio	2. ratio	a	b
$^3He/^4He$	$^6Li/^7Li$	2.18	13.33
	$^7Li/^8Li$	1.98	18.54
	$^9Be/^{10}Be$	0.38	13.77
	$^{10}B/^{11}B$	0.86	9.12
	$^{11}B/^{12}B$	1.11	17.21
$^6Li/^7Li$	$^7Li/^8Li$	0.91	5.22
	$^9Be/^{10}Be$	0.17	0.44
	$^{10}B/^{11}B$	0.39	-4.21
	$^{11}B/^{12}B$	0.51	3.88
$^7Li/^8Li$	$^9Be/^{10}Be$	0.19	-4.78
	$^{10}B/^{11}B$	0.43	-9.42
	$^{11}B/^{12}B$	0.56	-1.34
$^9Be/^{10}Be$	$^{10}B/^{11}B$	2.25	-4.64
	$^{11}B/^{12}B$	2.92	3.44
$^{10}B/^{11}B$	$^{11}B/^{12}B$	1.30	8.09

Table 1: Constants a and b entering into Eq.2 for different combinations of isotope pairs.

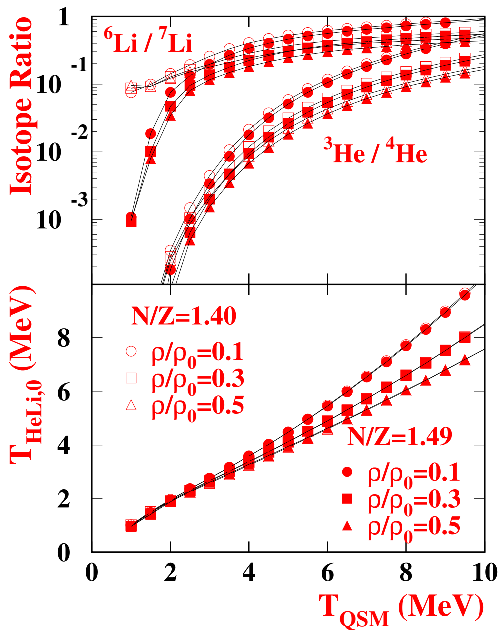

Figure 3: Single isotope ratios (top part) and $T_{HeLi,0}$ (bottom part) calculated from the fragment distribution of the QSM model [41, 42] as a function of the initial temperature.

the relative variation of the temperature for a relative change of the double ratio R can be written as

$$\frac{\Delta T}{T} = -\frac{T}{b}\frac{\Delta R}{R}. \tag{4}$$

Assuming a typical temperature of 5 MeV, a modification of R by $\pm 50\%$ causes a change of the extracted temperature $T_{HeLi,0}$ by only $\mp 19\%$ or $\Delta T = \mp 1.0$ MeV.

4 Calibration of the Temperature Scale

In order to test the model dependence of the temperature definition via Eq.3 and to investigate the influence of sequential decays we analyzed the fragment distributions predicted by several decay models.

Isotope ratios of $^6Li/^7Li$ and $^3He/^4He$ calculated by the quantum statistical model (QSM) [41, 42] are shown in the upper part of Fig. 3 as a function of the initial temperature T_{QSM}. Both, the breakup density ρ/ρ_0 and the N/Z ratio of the initial system, influence the individual isotope ratios. Evaluating, however, the double-ratio (or $T_{HeLi,0}$) the influence of the N/Z ratio of the emitting system cancels nearly completely and the uncertainty of T_{QSM} due to variations of the breakup density is reduced by roughly a factor of two as compared to the case where the temperature would have been determined e.g. from the $^3He/^4He$ ratio alone (lower part of Fig. 3). Despite the strong feeding of the light particle yields through secondary decays the QSM calculations predict an almost linear dependence of $T_{HeLi,0}$ on the actual temperature T of the system. For temperatures below 10 MeV, the ratio $T_{HeLi,0}$/T varies between about 0.95±0.05 and 0.75±0.05 for breakup densities between $0.1 \cdot \rho_0$ and $0.5 \cdot \rho_0$.

Results of sequential evaporation calculations with the code GEMINI [43] also confirm a nearly linear relation between $T_{HeLi,0}$ and the *initial* temperature of the system $T = \sqrt{k \cdot \langle E_0 \rangle / \langle A_0 \rangle}$, where k denotes the inverse level density parameter (see stars in Fig. 4). In line with QSM calculations for higher densities the ratio $T_{HeLi,0}/T \approx 0.7$. Finally, also the microcanonical multifragmentation model of Gross and co-workers [23] predicts a rather constant ratio of 0.7±0.05 between $T_{HeLi,0}$ and the thermodynamic temperature of the system (solid dots in Fig. 4).

In order to account pragmatically for the systematic underestimation of the temperature by the quantity $T_{HeLi,0}$, we define the final isotope temperature via

$$T_{HeLi} = 1.2 \cdot T_{HeLi,0}. \tag{5}$$

Thus, T_{HeLi} provides - within the models mentioned and within ±15% - a common temperature scale in the evaporation, fragmentation as well as in the vapor regime of nuclear systems.

5 The Caloric Curve of Nuclei

Figure 5 shows the isotope temperature as a function of the total excitation energy per nucleon. As described in the contribution of W. Trautmann to this meeting [37] the excitation energies were determined by a total energy balance as suggested by Campi and co-workers [44]. We would like to stress that the isotope thermometer and the excitation energies are practically independent observables, thus avoiding auto-correlations when plotted against each other.

Excitation energy - temperature pairs of this caloric curve extracted for projectile spectators of Au+Au collisions at E/A=600 MeV are marked by the solid points. Data for target residues produced at intermediate energies between E/A=30 and 84 MeV are shown by the open squares. In the latter case, the excitation energies were also deduced from an energy balance [45] and T_{HeLi} was evaluated using the coincident light particle yields associated with emission from the target remnant [46]. Because of the finite width of the

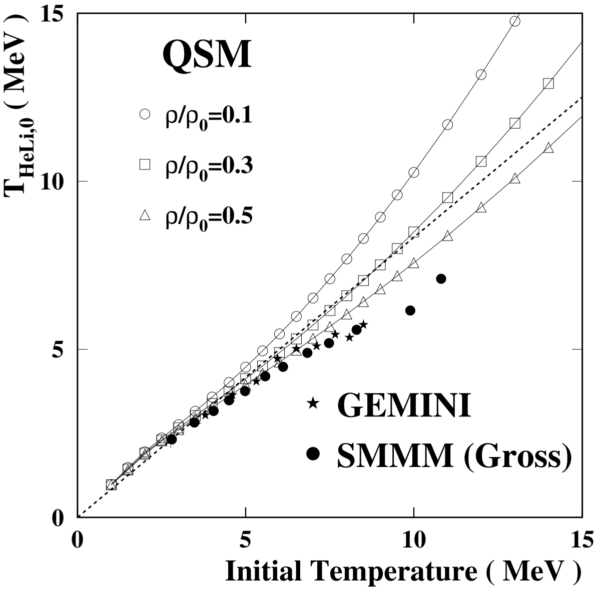

Figure 4: T_{HeLi} calculated from fragment distributions of different decay models as a function of the initial temperature.

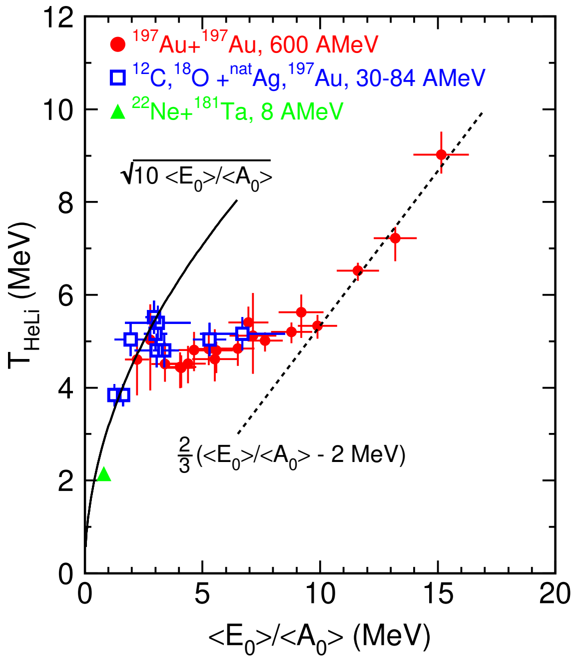

Figure 5: Caloric curve of nuclei determined by the dependence of the isotope temperature T_{HeLi} on the excitation energy per nucleon. The lines are explained in the text.

excitation energy distribution and the exponentially decreasing production rate of ^{3}He towards low excitation energies temperatures can not be determined for excitation energies below approximately 2 MeV per nucleon in the present study. The only value for T_{HeLi} in the evaporation regime below 2 MeV per nucleon excitation energy is provided by the ^{22}Ne+^{181}Ta fusion reactions at E/A=8.1 MeV [47] and is marked by the triangle in Fig. 5.

The caloric curve shown in Fig. 5 can be divided in three distinctly different sections. In line with previous studies in the fusion evaporation regime [48, 49] the rise of T_{HeLi} for excitation energies below 2 MeV per nucleon is compatible with the low-temperature approximation of a fermionic system

$$T = \sqrt{k \cdot \langle E_0 \rangle / \langle A_0 \rangle}. \tag{6}$$

For orientation, the solid line depicts relation (6) for an inverse level density parameter of k=10 MeV. Within the range of $\langle E_0 \rangle / \langle A_0 \rangle$ from 3 MeV to 10 MeV an almost constant value for T_{HeLi} of about 4.5-5 MeV is observed. This plateau may be related to the finding of rather constant emission temperatures over a broad range of incident energies which were deduced from the population of particle unstable levels in He and Li fragments [50]. We also note that the mean excitation energy of the plateau coincides with the limiting excitation energy for the fusion-evaporation process of about 4.5-6.4 MeV per nucleon [51]. Finally, beyond a total excitation energy of 10 MeV per nucleon, a steady rise of T_{HeLi} with increasing $\langle E_0 \rangle / \langle A_0 \rangle$ is seen which may be described by a linear relation

$$T_{HeLi} = 2/3 \cdot (\langle E_0 \rangle / \langle A_0 \rangle - 2MeV) \tag{7}$$

where the slope of 2/3 alludes to a gas of classical, elementary particles.

The offset in eq. (7) probably signals a freeze out at a finite density. Assuming, for simplicity, a parabolic shape for the low density equation-of-state of the finite nuclear system [52]

$$(E/A)_{T=0} = K_c/18 \cdot (1 - \rho/\rho_0)^2 - 8MeV \tag{8}$$

and adding the excitation energy for a Fermi-Dirac gas at finite density, the data in the vapor regime at $\langle E_0 \rangle / \langle A_0 \rangle > 10$ MeV can be explained with a constant freeze-out density between ρ/ρ_0=0.15 and 0.3 if the compressibility K_c is varied between 144 and 300 MeV. While this interplay between the expansion dynamics and the density dependent properties of a Fermi gas might help to elucidate the gross features of the vapor branch, one has to keep in mind that also in this regime typically 20% of the mass of the decaying system is contained in intermediate mass fragments. An internally consistent equation-of-state taking into account the formation of clusters [29], the particle loss during the expansion [26, 28] and the systematic variation of the source size [37] is therefore required before more definite conclusions can be drawn.

The plateau of the caloric curve in Fig. 5 is suggestive of a first-order phase transition with a substantial latent heat. It also seems to exclude - on first sight - the occurence of a second-order phase transition which is the *sine qua non* for the determination of critical-point exponents [14, 15] (see also the contribution of W.F.J. Müller to this conference). For a finite system with N constituents a transition is, on the other hand, no longer characterized by a singular point but acquires a finite width over a temperature range ΔT_c around the transition temperature T_c. In case of a second order phase transition, $\Delta T_c/T_c$ is approximately given by $\Delta T_c/T_c \sim 1/\sqrt{N}$ [16]. For typical nuclear sizes of N≈100, the influence of a second order phase transition may, therefore, be perceptible at temperatures deviating by as much as 10% from the critical value. Furthermore, for a classical van der Waals gas the latent heat increases close to the critical point with $\sqrt{1 - T/T_c}$ and reaches already at $T/T_c = 0.95$ values larger than $k_B T_c$. Thus, in finite systems typical features of a first-order phase transition - like a latent heat - and signals indicating the proximity of the critical point - like diverging moments - are not necessarily inconsistent.

In summary, we have studied fragment distributions resulting from projectile spectators in Au+Au collisions at an incident energy of E/A=600 MeV. From the observed fragment and neutron distributions, the masses and excitation energies of the decaying pre-fragments were determined. A temperature scale was derived from observed yield ratios of He and Li isotopes. Rising first strongly with increasing excitation energy, the isotope temperature stays rather constant at a value of about 5 MeV for excitation energies between 3 and 10 MeV per nucleon. For higher excitation energies, again an increasing temperature is found. Depending on the low density equation-of-state the freeze-out in this vapor regime may by characterized by a density between 0.15 and 0.3 of normal nuclear density. The observed caloric curve agrees qualitatively with predictions of the Copenhagen multifragmentation model [22] and is reminiscent of the paradigm of a phase transition, the first-order phase transition of bulk (and also finite [32]) H_2O - systems. Nonetheless, a transition in close proximity to the critical point can not be excluded for this finite system, making the attempt to extract critical-point exponents - at least - a worthwhile and interesting venture.

We thank J. Konopka for providing us with the results of the QSM calculations. J.P. and M.B. acknowledge the financial support of the Deutsche Forschungsgemeinschaft under the Contract No. Po256/2-1 and No. Be1634/1-1, respectively. This work was supported in part by the European Community under contract ERBCHGE-CT92-0003 and ERBCIPD-CT94-0091.

References

[1] D.Q. Lamb *et al.*, Phys. Rev. Lett. P**41**, 1623 (1978).

[2] H. Jaqaman, A.Z. Mekjian, and L. Zamick, Phys. Rev. C **27**, 2782 (1983) and Phys. Rev. C **29**, 2067 (1984).

[3] L. Satpathy, M. Mishra, and R. Nayak, Phys. Rev. C **39**, 162 (1989).

[4] J.E. Finn *et al.*, Phys. Rev. Lett. **49**, 1321 (1982).

[5] J. Kapusta, Phys. Rev. C **29**, 1735 (1984).

[6] A.L. Goodman, J. Kapusta, and A.Z. Mekjian, Phys. Rev C **30**, 851 (1984).

[7] D.H. Boal and A.L. Goodman, Phys. Rev. C **33**, 1690 (1986).

[8] M.E. Fisher, Physics **3**, 255 (1967).

[9] P.J. Siemens, Nature **305**, 410 (1983).

[10] A.D. Panagiotou *et al.*, Phys. Rev. Lett. **52**, 496 (1984).

[11] C.B. Chitwood *et al.*, Phys. Lett. **131B**, 289 (1983).

[12] J. Hüfner and D. Mukhopadhyay, Phys. Lett. B **173**, 373 (1986).

[13] R. Botet and M. Ploszajczak, Int. J. Mod. Phys. **E3**, 1033 (1994) and references therein.

[14] M.L. Gilkes *et al.*, Phys. Rev. Lett. **73**, 1590 (1994).

[15] J.B. Elliott *et al.*, Phys. Rev. C **49**, 3185 (1994).

[16] Y. Imry, Phys. Rev. B **21**, 2042 (1980).

[17] P. Labastie and R.L. Whetten, Phys. Rev. Lett. **65**, 1567 (1990).

[18] D.H. Boal and J.N. Glosli, Phys. Rev. C **42**, R502 (1990).

[19] Wang Neng-ping, Yang Shan-de, and Xu Gong-ou, J. Phys. G **20**, 101 (1994).

[20] G.T. Zheng, Phys. Rev C **50**, 771 (1994).

[21] S. Levit and P. Bonche, Nucl. Phys. **A437**, 426 (1985).

[22] J. Bondorf *et al.*, Nucl. Phys. A **444**, 460 (1985).

[23] D.H.E. Gross, Prog. Part. Nucl. Phys. **30**, 155 (1993).

[24] G. Bertsch and P.J. Siemens, Phys. Lett. **126B**, 9 (1983).

[25] J.A. Lopez and P.J. Siemens, Nucl. Phys. **A431**, 728 (1984).

[26] W.A. Friedman, Phys. Rev. C **42**, 667 (1990).

[27] M. Belkacem, V. Latora, and A. Bonasera, Phys. Lett. B **326**, 21 (1994).

[28] G. Papp and W. Nörenberg, Proceedings of the International Workshop XXII on Gross Properties of Nuclei and Nuclear Excitations, Hirschegg 1994, p. 87.

[29] G. Peilert *et al.*, Phys. Lett. B **260**, 271 (1991).

[30] H.-P. Cheng *et al.*, Phys. Rev. A **46**, 791 (1992).

[31] A. Hüller, Z. Phys. B **93**, 401 (1994).

[32] D.J. Wales and I. Ohmine, J. Chem. Phys. **98**, 7245 (1993).

[33] R. Blümel *et al.*, Nature **334**, 309 (1988).

[34] J. Hubele *et al.*, Z. Phys. A **340**, 263 (1991); Phys. Rev. C **46**, R1577 (1992); P. Kreutz *et al.*, Nucl. Phys. **A556**, 672 (1993).

[35] G.J. Kunde *et al.*, Phys. Rev. Lett. **74**, 38 (1995).

[36] V. Lindenstruth, PhD thesis, University Frankfurt 1993, GSI-report GSI-93-18 (unpublished).

[37] W. Trautmann *et al.*, contribution to this meeting.

[38] J. Pochodzalla *et al.*, Nucl. Phys. **A583**, 553c (1995).

[39] Th. Blaich *et al.*, Nucl. Instr. and Method **A314**, 136 (1992).

[40] S. Albergo *et al.*, Nuovo Cimento A **89**, 1 (1985).

[41] D. Hahn and H. Stöcker, Nucl. Phys. **A476**, 718 (1988).

[42] J. Konopka *et al.*, Phys. Rev. C **50**, 2085 (1994).

[43] R.J. Charity *et al.*, Nucl. Phys. **A483**, 371 (1988).

[44] X. Campi, H. Krivine, and E. Plagnol, Phys. Rev. C **50**, R2680 (1994).

[45] R. Trockel *et al.*, Phys. Rev. C **39**, 729 (1989).

[46] R. Trockel, PhD thesis, University of Heidelberg 1988 (unpublished).

[47] C. Borcea *et al.*, Nucl. Phys. **A415**, 169 (1984).

[48] G. Nebbia *et al.*, Phys. Lett. B **176**, 20 (1986).

[49] D. Fabris *et al.*, Phys. Lett. B **196**, 429 (1987).

[50] G.J. Kunde *et al.*, Phys. Lett. B **272**, 202 (1991).

[51] W. Bohne *et al.*, Phys. Rev. C**41**, R5 (1990).

[52] W.A. Friedman, 8-th Winter Workshop on Nuclear Dynamics, Jackson Hole, Wyoming, January 1992.